



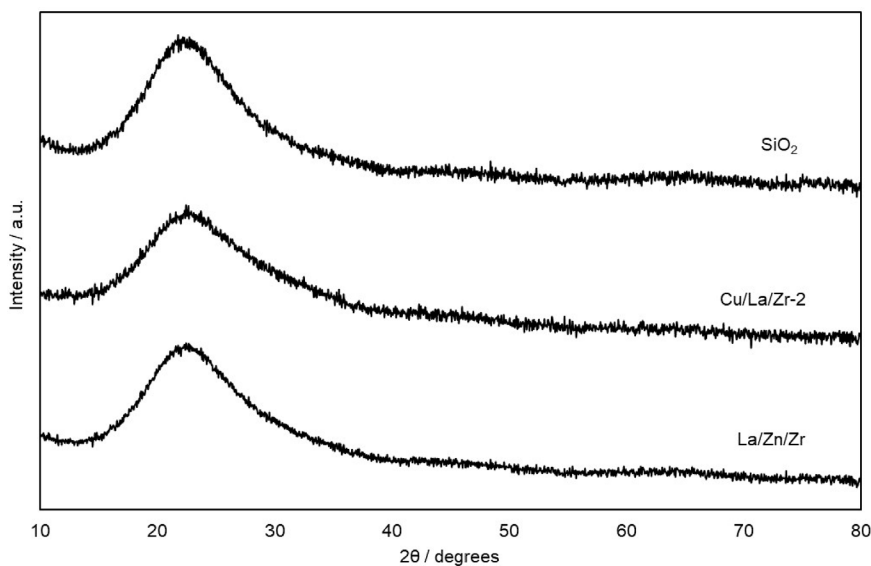
# Supplementary material: Investigations into the conversion of ethanol to butadiene-1,3 using CuO/La<sub>2</sub>O<sub>3</sub>/ZrO<sub>2</sub>/SiO<sub>2</sub> catalyst systems

Maxim Makhin<sup>\*, a</sup>, Stanislav Bedenko <sup>a</sup>, Alexey Budnyak <sup>a</sup>, Georgy Dmitriev <sup>a</sup> and Leonid Zhanaveskin <sup>a</sup>

<sup>a</sup> A.V. Topchiev Institute of Petrochemical Synthesis RAS, 119991, Leninsky Ave 29, Moscow, Russia

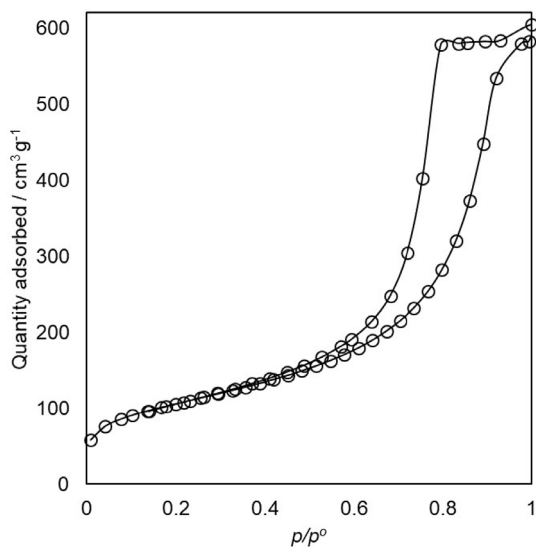
*E-mails:* Makhin.maxim@gmail.com (M. Makhin), bedenko@ips.ac.ru (S. Bedenko), budnyak@ips.ac.ru (A. Budnyak), dmitriev.gs@ips.ac.ru (G. Dmitriev), zhanaveskin@ips.ac.ru (L. Zhanaveskin)

*Manuscript received 15 June 2022, revised 5 November 2022, accepted 15 December 2022.*

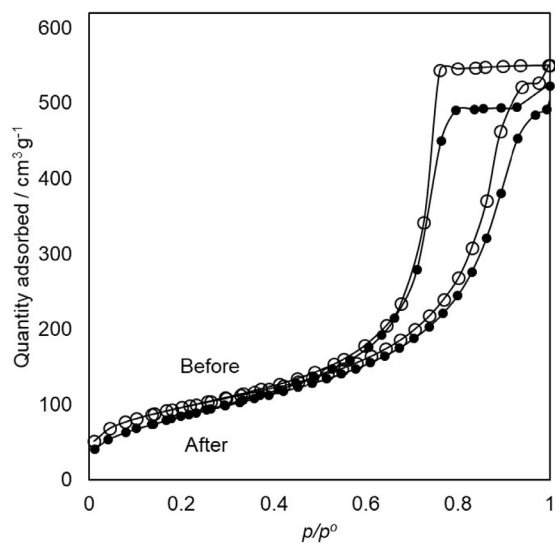


**Supplementary Figure S1.** XRD patterns of SiO<sub>2</sub>, La/Zn/Zr and Cu/La/Zr-2.

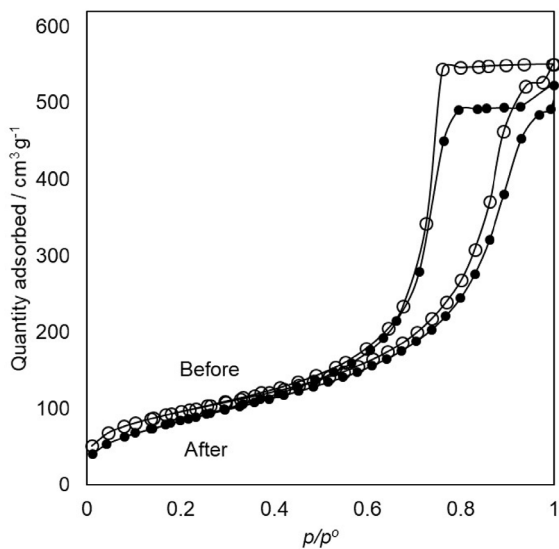
\* Corresponding author.



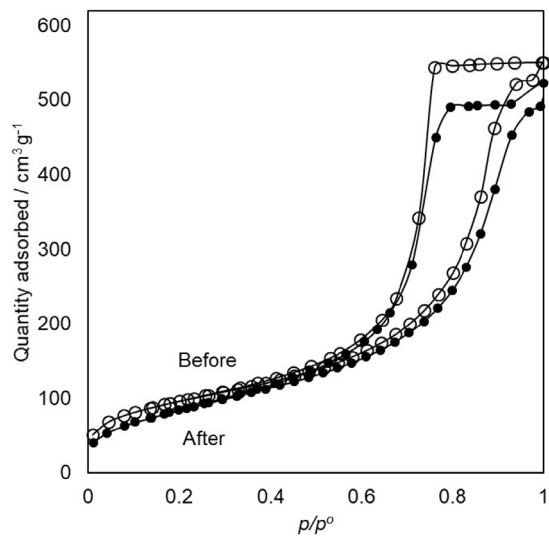
**Supplementary Figure S2.** Isotherm of nitrogen physisorption on SiO<sub>2</sub>.



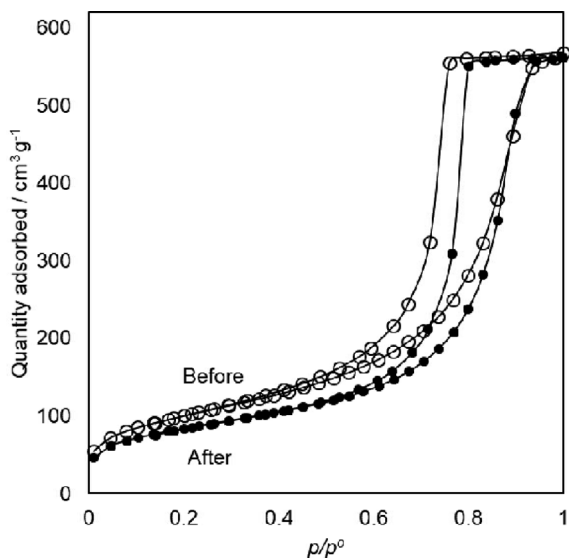
**Supplementary Figure S4.** Isotherm of nitrogen physisorption on Cu/Zn/Zr before and after the experiment.



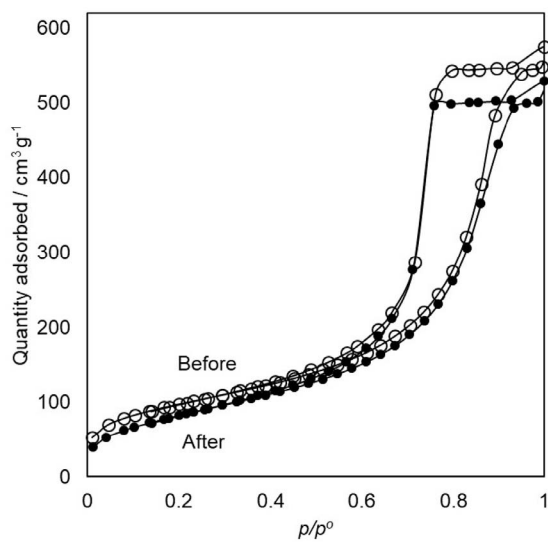
**Supplementary Figure S3.** Isotherm of nitrogen physisorption on Zn/Zr before and after the experiment.



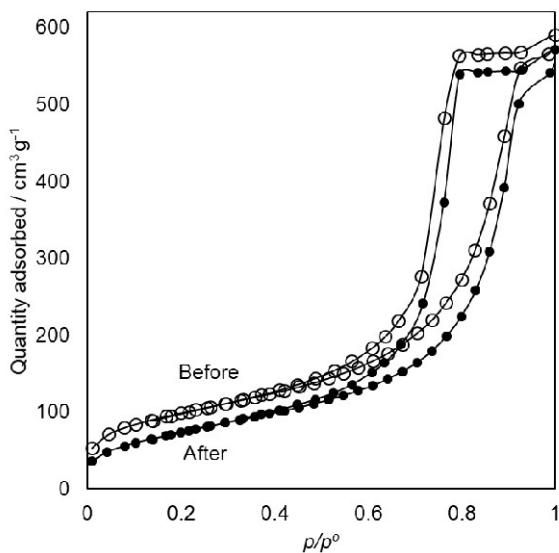
**Supplementary Figure S5.** Isotherm of nitrogen physisorption on La/Zn/Zr before and after the experiment.



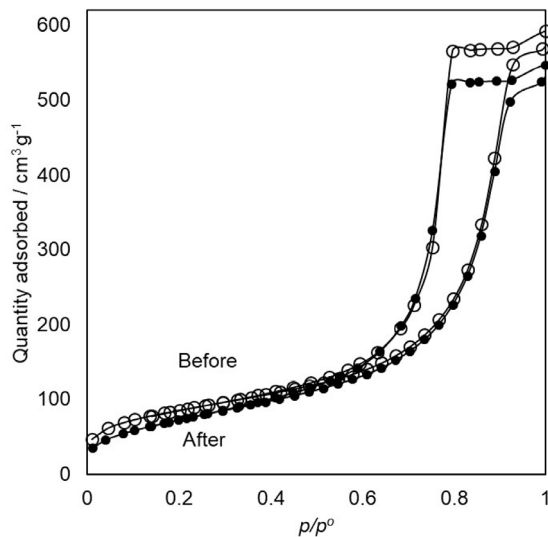
**Supplementary Figure S6.** Isotherm of nitrogen physisorption on Cu/La/Zr-1 before and after the experiment.



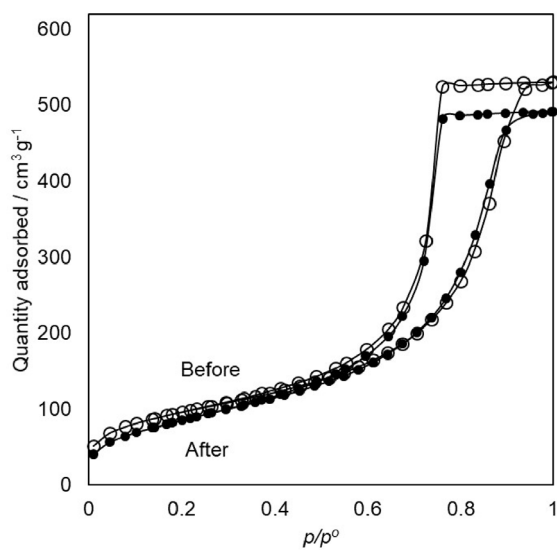
**Supplementary Figure S8.** Isotherm of nitrogen physisorption on Cu/La/Zr-3 before and after the experiment.



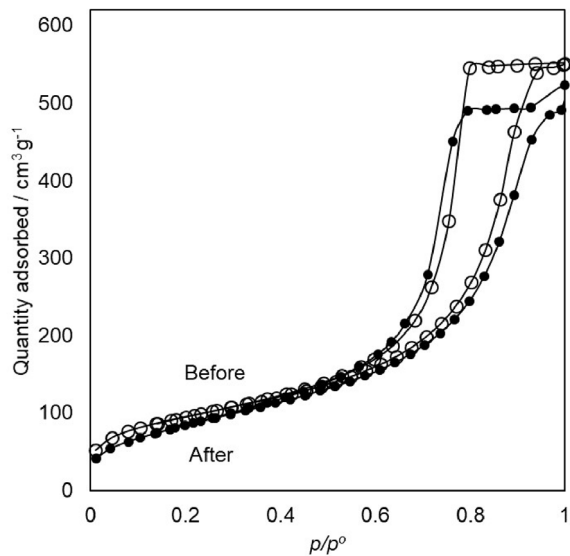
**Supplementary Figure S7.** Isotherm of nitrogen physisorption on Cu/La/Zr-2 before and after the experiment.



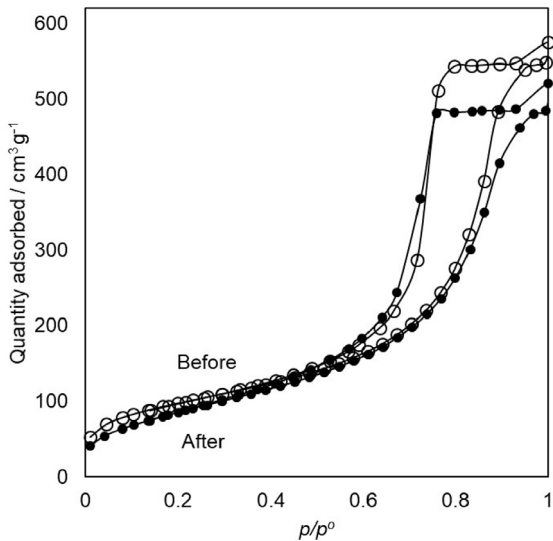
**Supplementary Figure S9.** Isotherm of nitrogen physisorption on Cu/La/Zr-4 before and after the experiment.



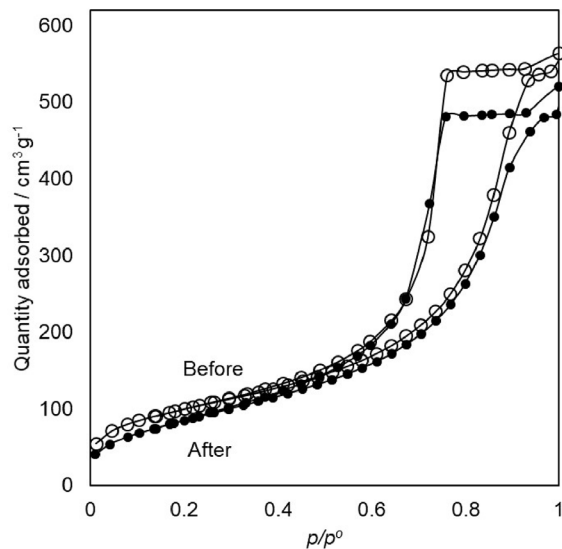
**Supplementary Figure S10.** Isotherm of nitrogen physisorption on Cu/La/Zr-5 before and after the experiment.



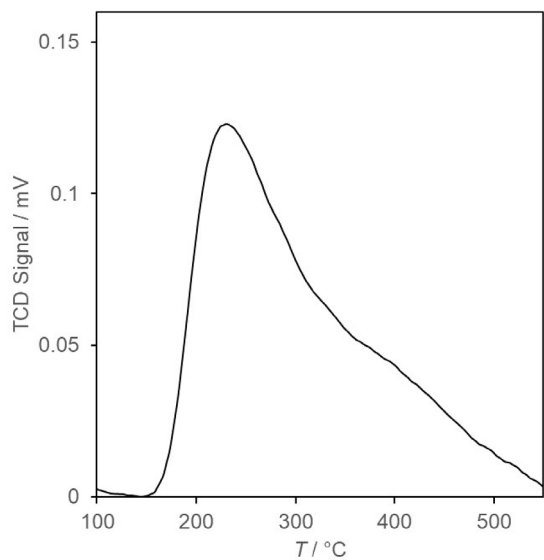
**Supplementary Figure S12.** Isotherm of nitrogen physisorption on Cu/La/Zr-7 before and after the experiment.



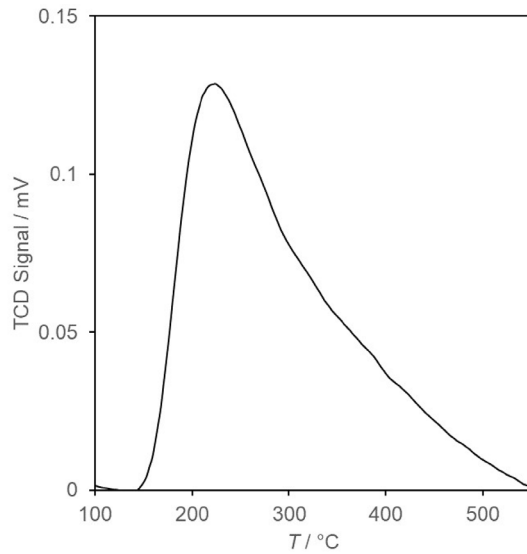
**Supplementary Figure S11.** Isotherm of nitrogen physisorption on Cu/La/Zr-6 before and after the experiment.



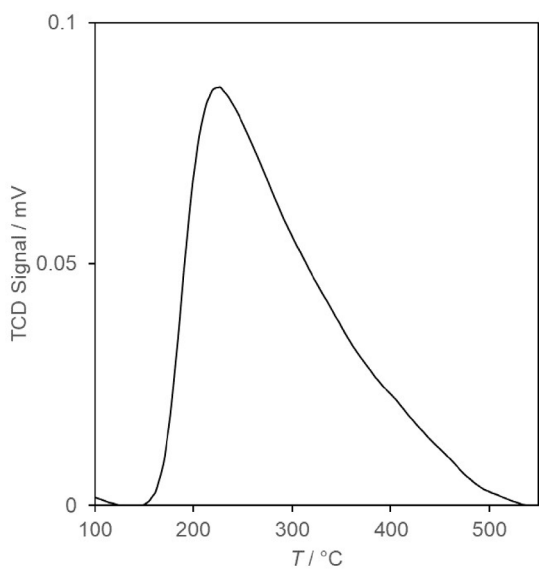
**Supplementary Figure S13.** Isotherm of nitrogen physisorption on Cu/La/Zr-8 before and after the experiment.



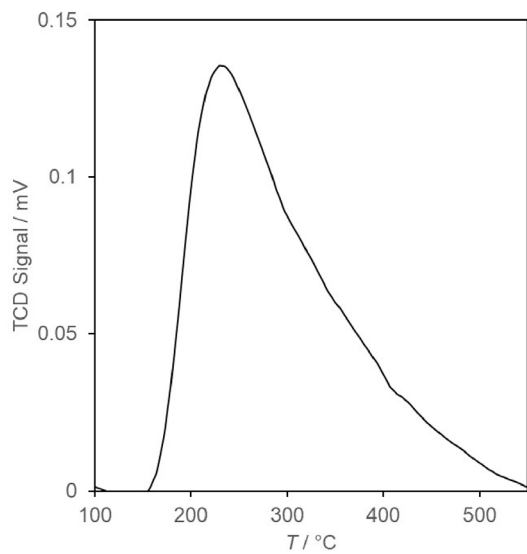
**Supplementary Figure S14.** The TPD-NH<sub>3</sub> curve (SiO<sub>2</sub>).



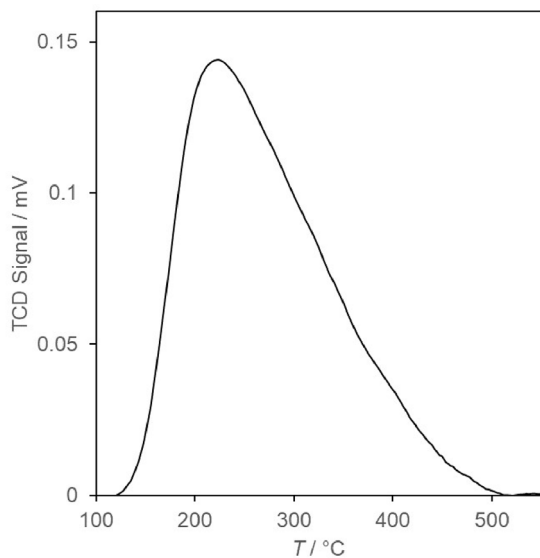
**Supplementary Figure S16.** The TPD-NH<sub>3</sub> curve (Cu/Zn/Zr).



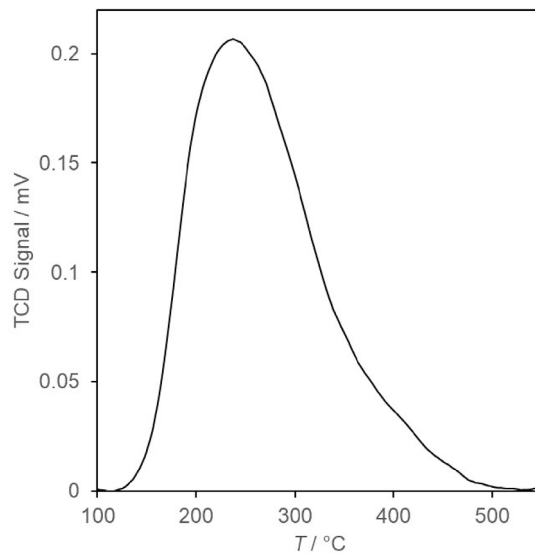
**Supplementary Figure S15.** The TPD-NH<sub>3</sub> curve (Zn/Zr).



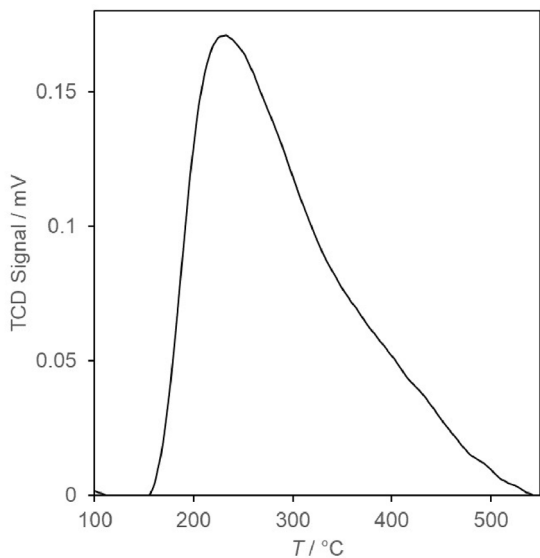
**Supplementary Figure S17.** The TPD-NH<sub>3</sub> curve (La/Zn/Zr).



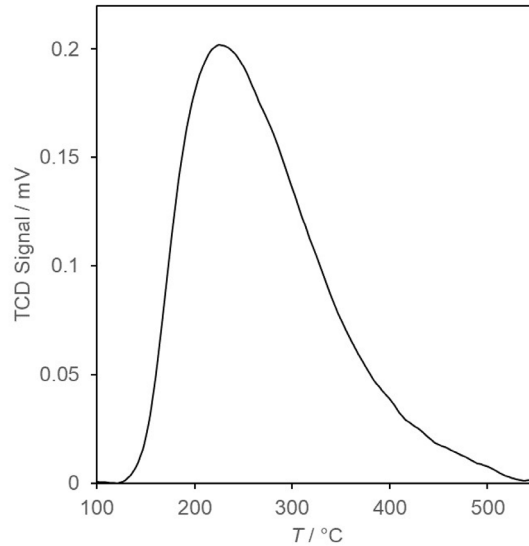
**Supplementary Figure S18.** The TPD-NH<sub>3</sub> curve (Cu/La/Zr-1).



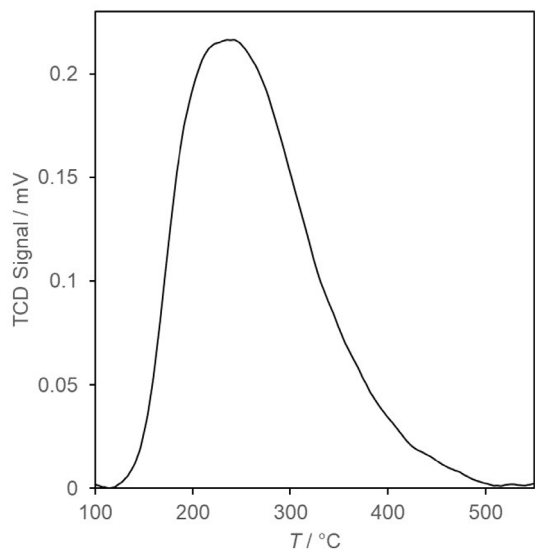
**Supplementary Figure S20.** The TPD-NH<sub>3</sub> curve (Cu/La/Zr-3).



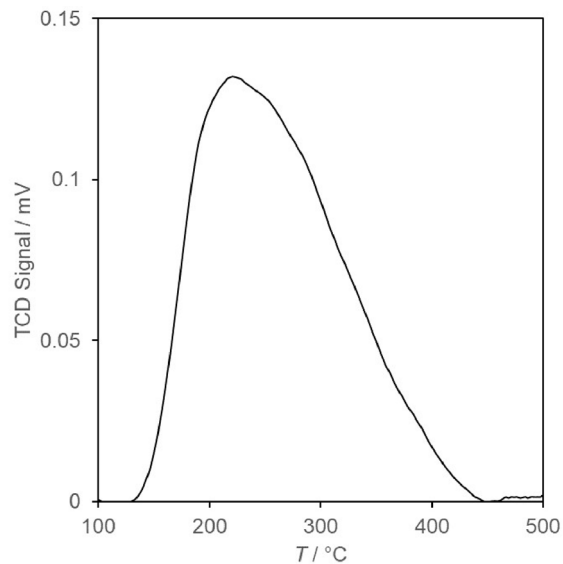
**Supplementary Figure S19.** The TPD-NH<sub>3</sub> curve (Cu/La/Zr-2).



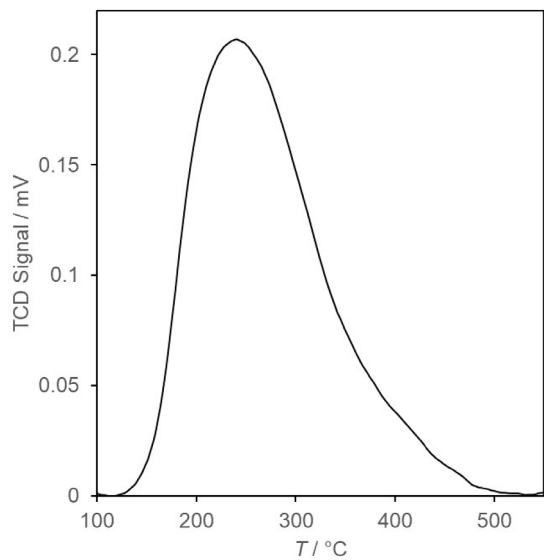
**Supplementary Figure S21.** The TPD-NH<sub>3</sub> curve (Cu/La/Zr-4).



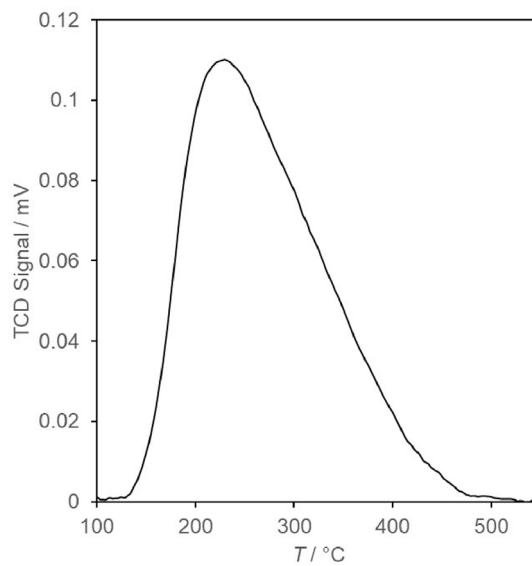
**Supplementary Figure S22.** The TPD-NH<sub>3</sub> curve (Cu/La/Zr-5).



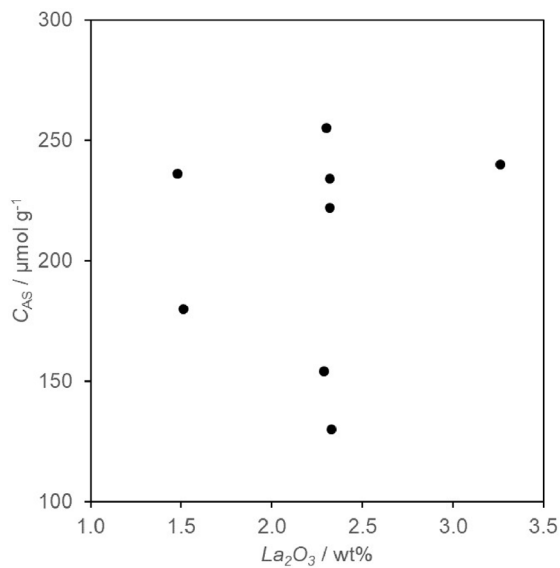
**Supplementary Figure S24.** The TPD-NH<sub>3</sub> curve (Cu/La/Zr-7).



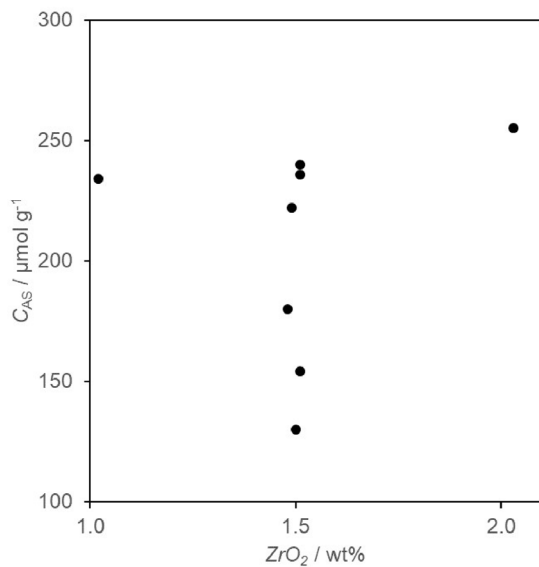
**Supplementary Figure S23.** The TPD-NH<sub>3</sub> curve (Cu/La/Zr-6).



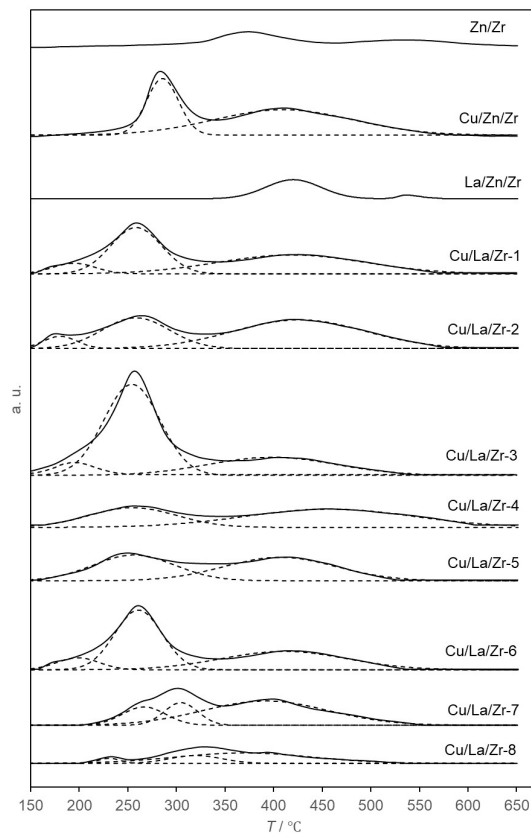
**Supplementary Figure S25.** The TPD-NH<sub>3</sub> curve (Cu/La/Zr-8).



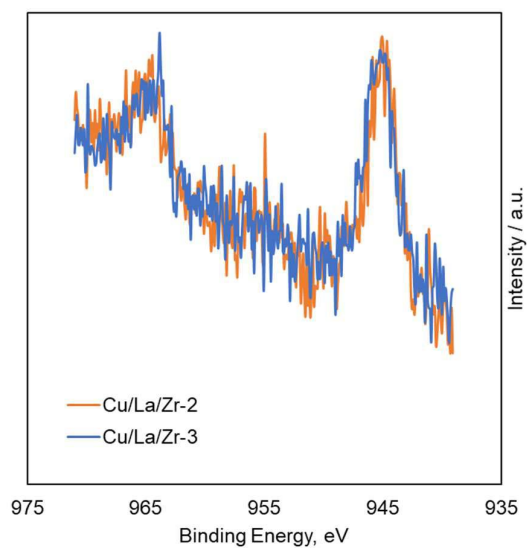
**Supplementary Figure S26.** Acid site concentration as a function of lanthanum content in Cu/La/Zr catalysts.



**Supplementary Figure S27.** Acid site concentration as a function of zirconium content in Cu/La/Zr catalysts.

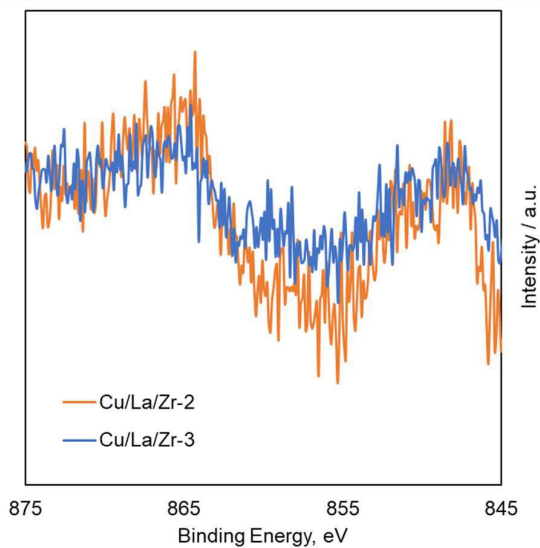


**Supplementary Figure S28.** The TPR curve for catalyst samples.

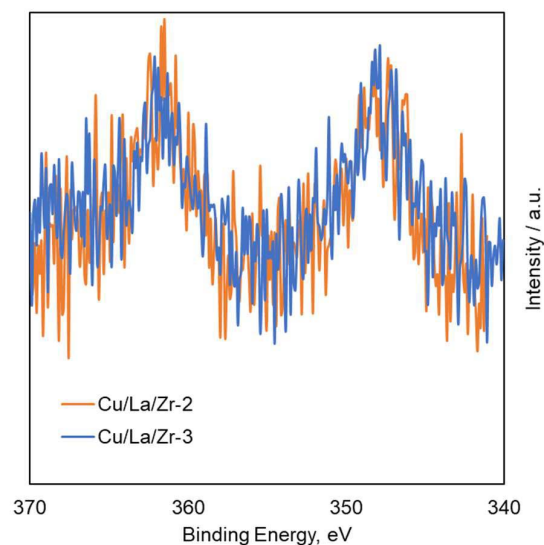


**Supplementary Figure S29.** XPS analysis of samples Cu/La/Zr-2 and Cu/La/Zr-3 (narrow scan of Cu).

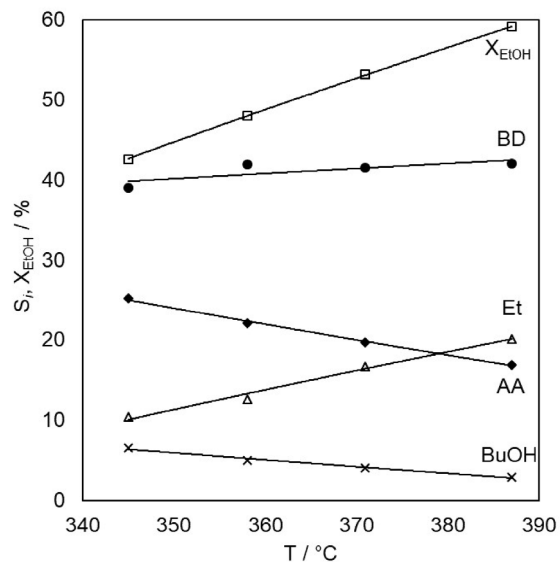




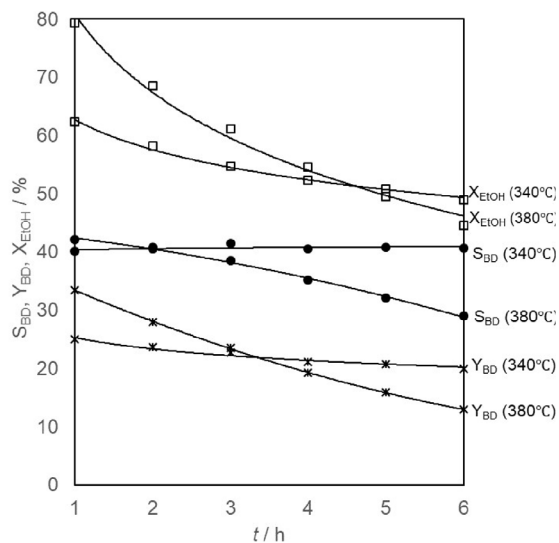
**Supplementary Figure S30.** XPS analysis of samples Cu/La/Zr-2 and Cu/La/Zr-3 (narrow scan of La).



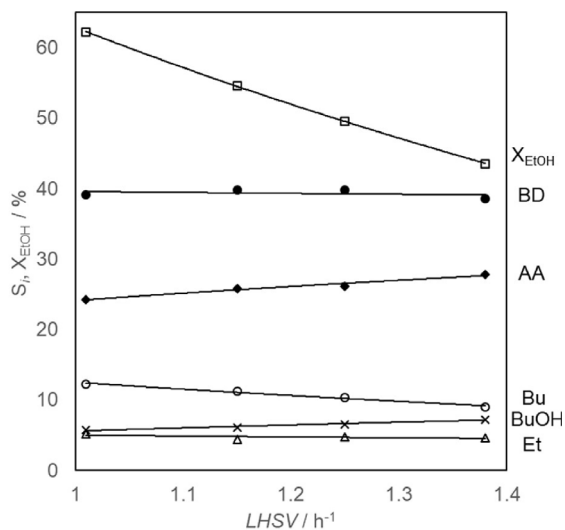
**Supplementary Figure S31.** XPS analysis of samples Cu/La/Zr-2 and Cu/La/Zr-3 (narrow scan of Zr).



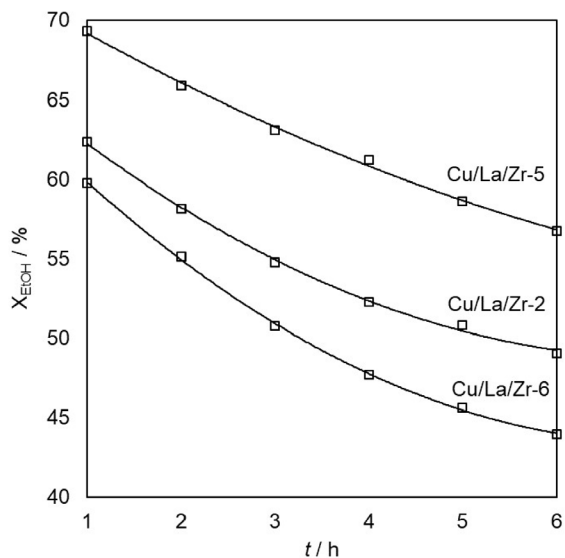
**Supplementary Figure S32.** Ethanol conversion and selectivity of the main reaction products as a function of temperature (100 cm<sup>3</sup> Cu/La/Zr-1, 340 °C,  $LHSV = 1.15 \text{ h}^{-1}$ ,  $t = 1 \text{ h}$ ).



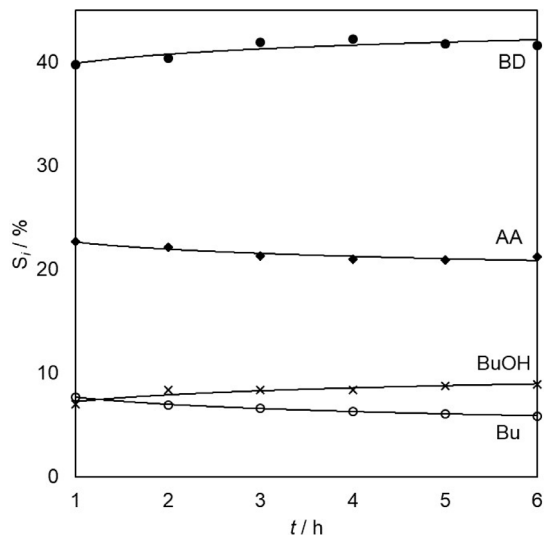
**Supplementary Figure S33.** Ethanol conversion, yield and selectivity butadiene as a function of time-on-stream at temperature 340 and 380 °C (100 cm<sup>3</sup> Cu/La/Zr-2,  $LHSV = 1 \text{ h}^{-1}$ ).



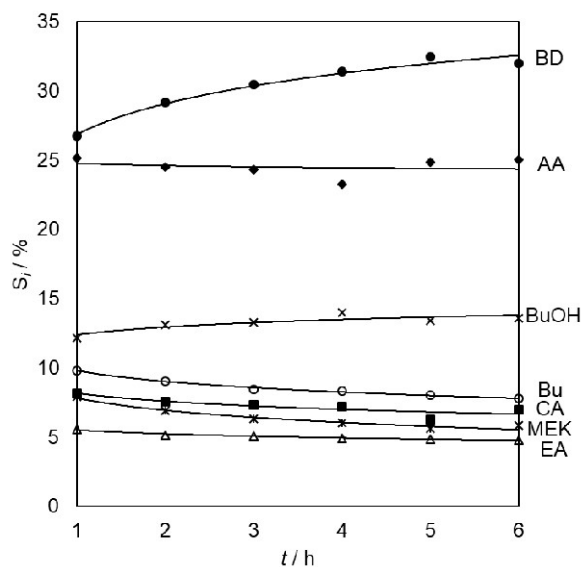
**Supplementary Figure S34.** Ethanol conversion and selectivity of the main reaction products as a function of  $LHSV$  ( $100 \text{ cm}^3$  Cu/La/Zr-2,  $340^\circ\text{C}$ ,  $t = 1 \text{ h}$ ).



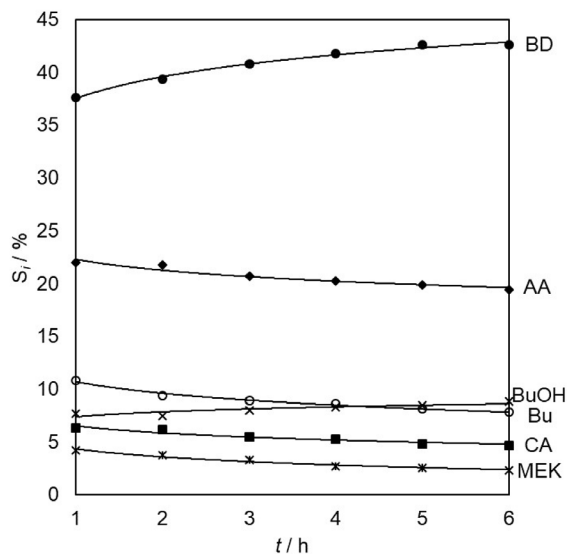
**Supplementary Figure S36.** Ethanol conversion as a function of time-on-stream over the Cu/La/Zr catalysts with different content Zr ( $100 \text{ cm}^3$  catalyst,  $340^\circ\text{C}$ ,  $LHSV = 1 \text{ h}^{-1}$ ).



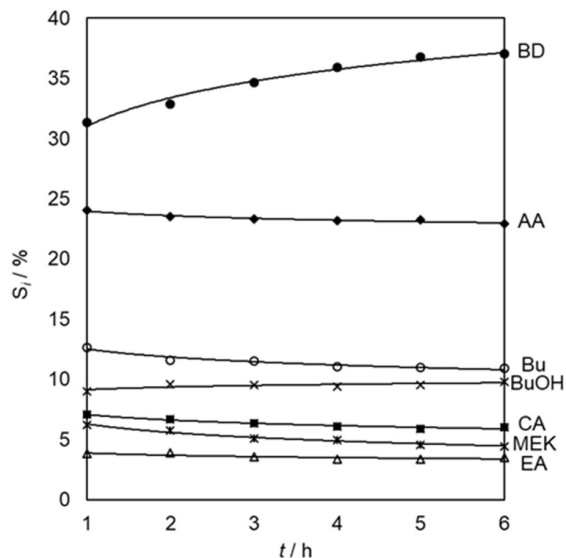
**Supplementary Figure S35.** Selectivity of the main reaction products as a function of time-on-stream ( $100 \text{ cm}^3$  Cu/La/Zr-6,  $340^\circ\text{C}$ ,  $LHSV = 1 \text{ h}^{-1}$ ).



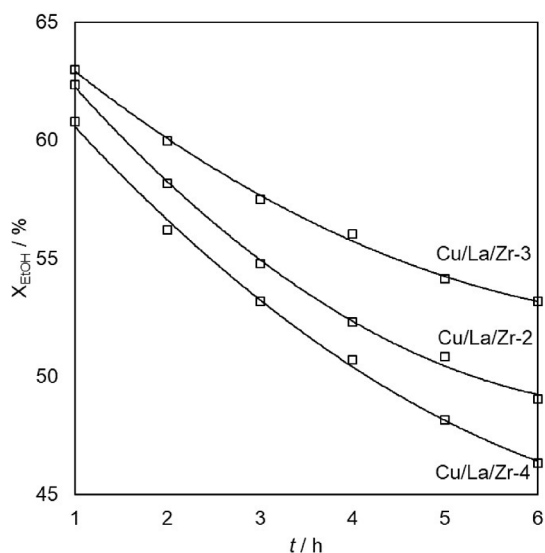
**Supplementary Figure S37.** Selectivity of the main reaction products as a function of time-on-stream ( $100 \text{ cm}^3$  Cu/La/Zr-5,  $340^\circ\text{C}$ ,  $LHSV = 1 \text{ h}^{-1}$ ).



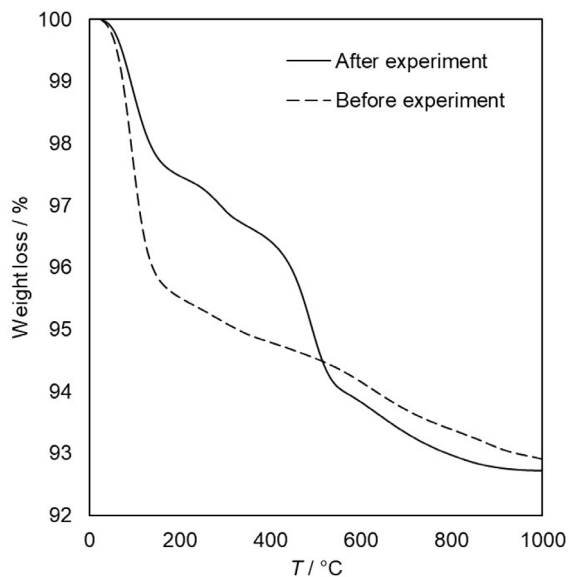
**Supplementary Figure S38.** Selectivity of the main reaction products as a function of time-on-stream ( $100 \text{ cm}^3 \text{ Cu/La/Zr-4}$ ,  $340 \text{ }^\circ\text{C}$ ,  $LHSV = 1 \text{ h}^{-1}$ ).



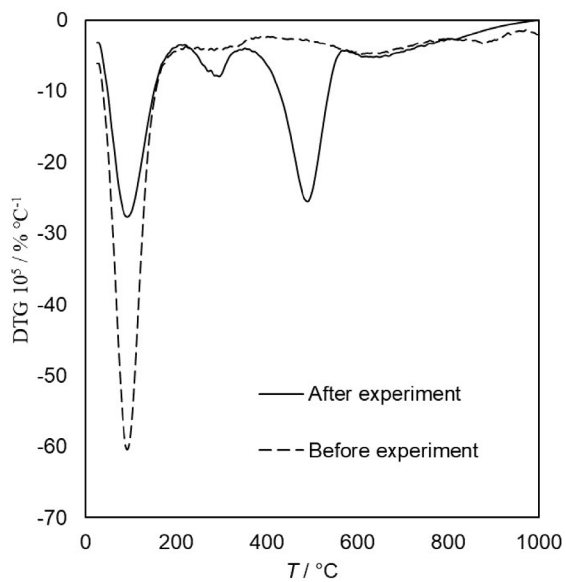
**Supplementary Figure S40.** Selectivity of the main reaction products as a function of time-on-stream ( $100 \text{ cm}^3 \text{ Cu/La/Zr-3}$ ,  $340 \text{ }^\circ\text{C}$ ,  $LHSV = 1 \text{ h}^{-1}$ ).



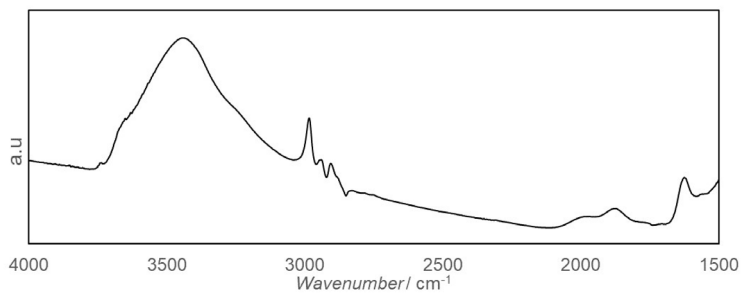
**Supplementary Figure S39.** Ethanol conversion as a function of time-on-stream over the Cu/La/Zr catalysts with different content La. ( $100 \text{ cm}^3 \text{ catalyst}$ ,  $340 \text{ }^\circ\text{C}$ ,  $LHSV = 1 \text{ h}^{-1}$ ).



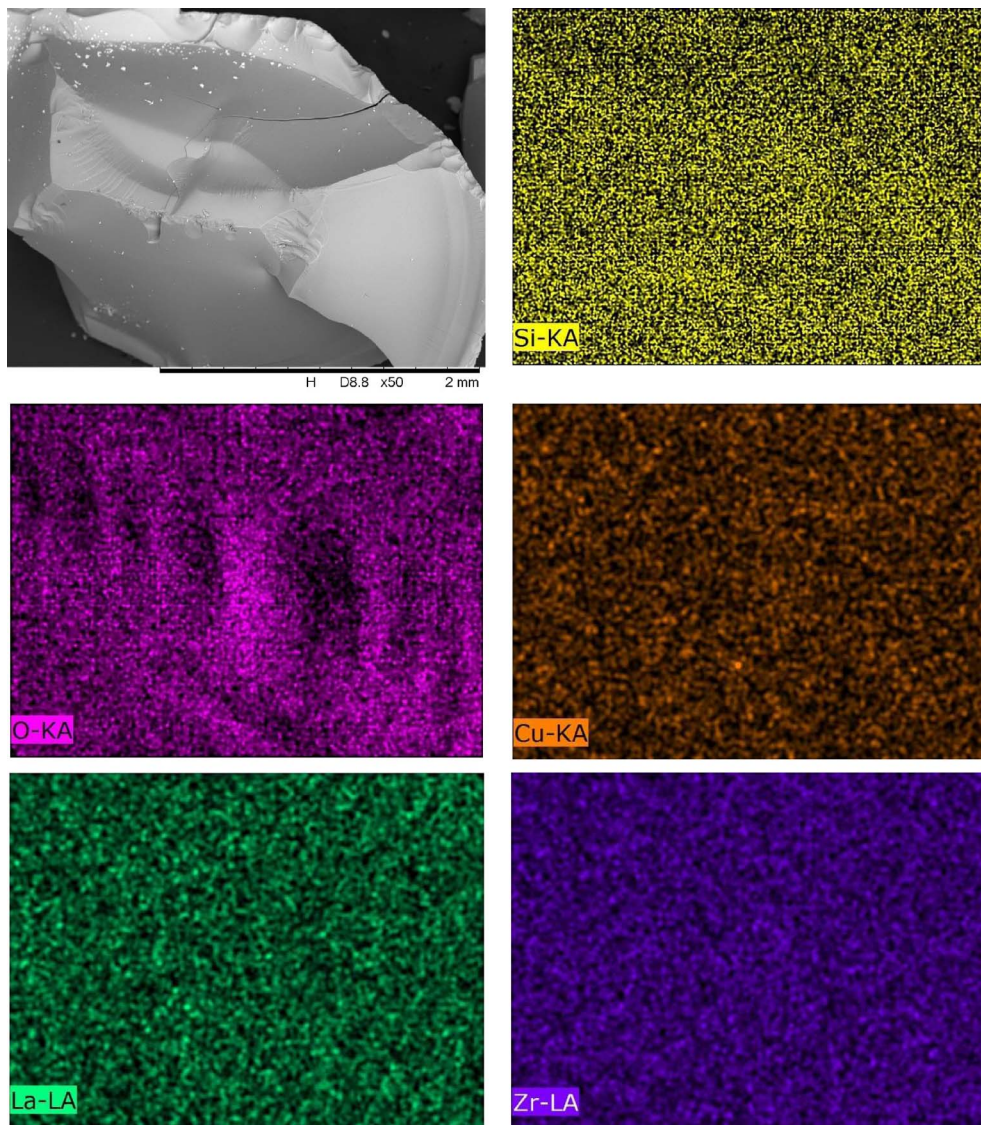
**Supplementary Figure S41.** TGA curves in air atmosphere for the Cu/La/Zr-2 before and after the experiment.



**Supplementary Figure S42.** DTG curves in air atmosphere for the Cu/La/Zr-2 before and after the experiment.

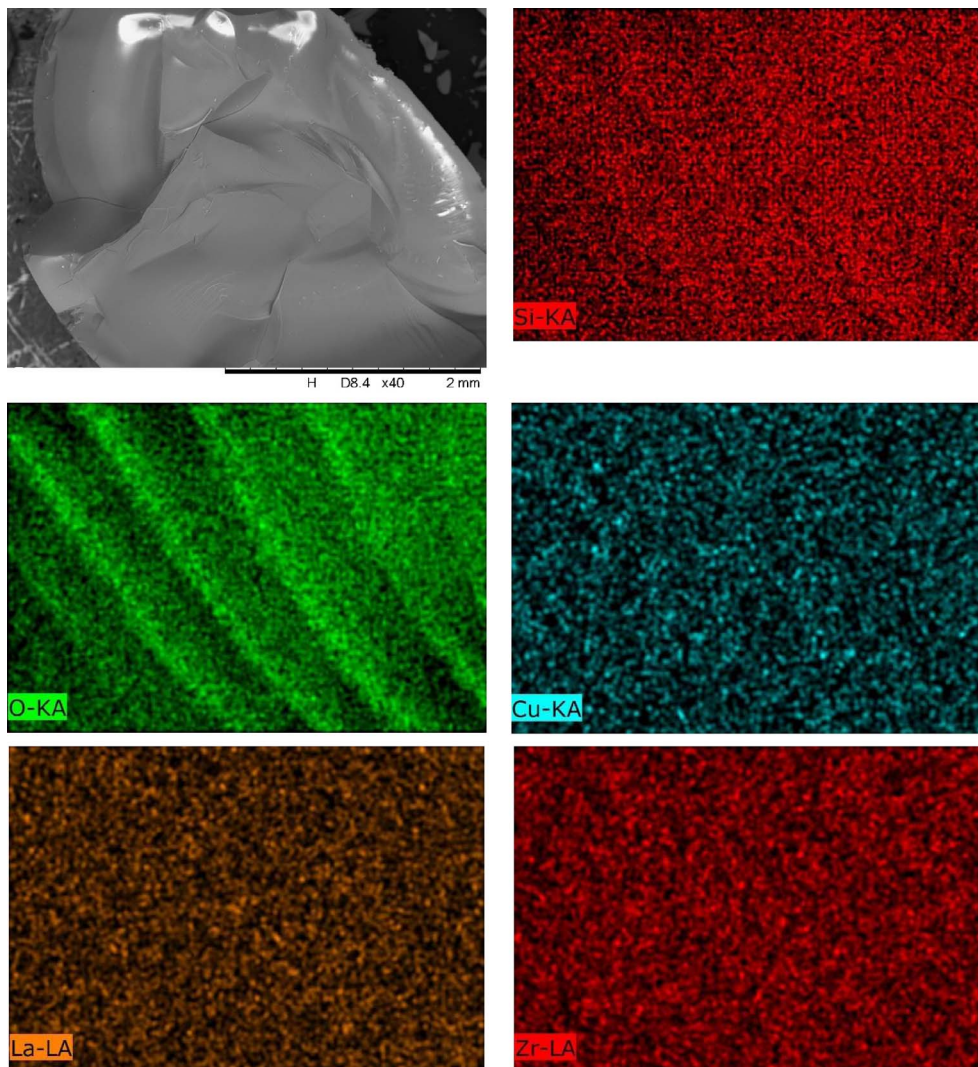


**Supplementary Figure S43.** FTIR result of coke deposit on the Cu/La/Zr-2.

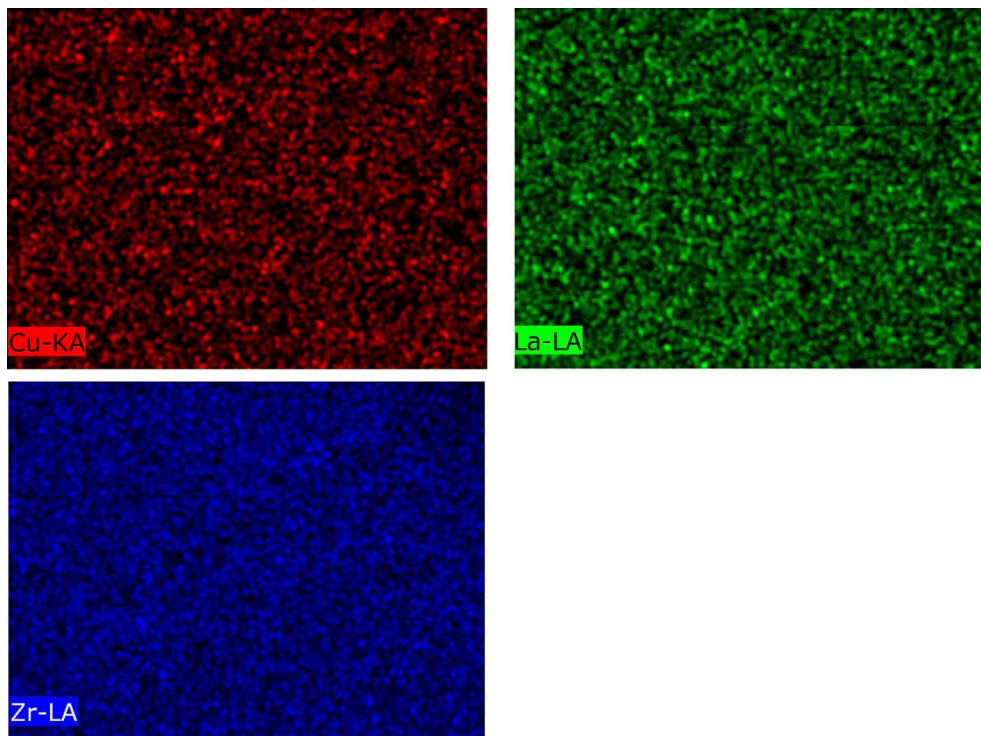


**Supplementary Figure S44.** Representative SEM image and element (Si, O, Cu, La, Zr) EDX mapping for the fresh Cu/La/Zr-2.





**Supplementary Figure S45.** Representative SEM image and element (Si, O, Cu, La, Zr) EDX mapping for the regenerated Cu/La/Zr-2.



**Supplementary Figure S46.** Element (Cu, La, Zr) EDX mapping for the fresh Cu/La/Zr-3.